Genome Medicine

RESEARCH

Open Access

Whole genome sequencing of 378 prostate cancer metastases reveals tissue selectivity for mismatch deficiency with potential therapeutic implications

Daniel J. Vis[1,2], Sander A. L. Palit[1], Marie Corradi[1], Edwin Cuppen[3,4,5], Niven Mehra[6], Martijn P. Lolkema[7], Lodewyk F. A. Wessels[2,5], Michiel S. van der Heijden[1,8*], Wilbert Zwart[5,9*] and Andries M. Bergman[8,9*]

Abstract

Background Survival of patients with metastatic castration-resistant prostate cancer (mCRPC) depends on the site of metastatic dissemination.

Methods Patients with mCRPC were prospectively included in the CPCT-02 metastatic site biopsy study. We evaluated whole genome sequencing (WGS) of 378 mCRPC metastases to understand the genetic traits that affect metastatic site distribution.

Results Our findings revealed that *RB1*, *PIK3CA*, *JAK1*, *RNF43*, and *TP53* mutations are the most frequent genetic determinants associated with site selectivity for metastatic outgrowth. Furthermore, we explored mutations in the non-coding genome and found that androgen receptor (AR) chromatin binding sites implicated in metastatic prostate cancer differ in mutation frequencies between metastatic sites, converging on pathways that impact DNA repair. Notably, liver and visceral metastases have a higher tumor mutational load (TML) than bone and lymph node metastases, independent of genetic traits associated with neuroendocrine differentiation. We found that TML is strongly associated with DNA mismatch repair (MMR)-deficiency features in these organs.

Conclusions Our results revealed gene mutations that are significantly associated with metastatic site selectivity and that frequencies of non-coding mutations at AR chromatin binding sites differ between metastatic sites. Immunotherapeutics are thus far unsuccessful in unselected mCRPC patients. We found a higher TML in liver and visceral metastases compared to bone and lymph node metastases. As immunotherapeutics response is associated with mutational burden, these findings may assist in selecting mCRPC patients for immunotherapy treatment based on organs affected by metastatic disease.

Trial registration number NCT01855477.

*Correspondence:
Michiel S. van der Heijden
ms.vd.heijden@nki.nl
Wilbert Zwart
w.zwart@nki.nl
Andries M. Bergman
a.bergman@nki.nl
Full list of author information is available at the end of the article

Keywords Prostate cancer, Metastases, Site selectivity, Mutations, Coding DNA, Non-coding DNA, Tumor mutational load, Immunotherapeutics

Background

Prostate cancer is the second most common malignancy in men, with globally over 1.3 million new diagnoses and 359,000 cancer-related deaths yearly [1]. Primary prostate cancer has an excellent prognosis. However, metastatic disease is generally incurable [2, 3]. After an initial response to androgen deprivation therapy, the condition will invariably progress to metastatic castration-resistant prostate cancer (mCRPC), which is associated with high morbidity and mortality [4]. Approximately 90% of patients with mCRPC will develop bone metastases during the course of the disease, rendering bone the most common site for prostate cancer metastases [5]. Lymph node (LN), liver, and (non-liver) visceral metastases are less frequent and commonly co-occur with bone metastases [5]. Importantly, there is a strong association between the sites of metastases and the prognosis of patients with disseminated prostate cancer. Patients with only LN metastases have the most favorable outcome. In contrast, patients with liver metastases have the worst prognosis, irrespective of concurrent metastases at other sites [6]. Moreover, several studies suggest differential responses of mCRPC metastatic sites to treatments [7, 8].

Cancer metastasis to specific organs occurs through a non-stochastic process termed metastatic organotropism, which is cancer-type specific and thought to be governed by interactions between the tumor cells and the tumor microenvironment at the pre-metastatic niche [9, 10]. Mediators of these interactions include genetic aberrations that alter growth and survival signals, metabolism, and the expression of cell surface markers and secreted factors [11–13]. The mutational inter-patient heterogeneity of prostate cancer metastases is also affected by the accumulation of genetic traits during the course of the disease and subsequent therapies [14, 15].

Androgen receptor (AR) is the pivotal hormone-driven transcription factor in prostate cancer development, and inhibiting its actions represents the most effective treatment of this disease. Upon testosterone binding, AR predominantly interacts with regulatory elements throughout the chromatin [16, 17]. Patterns of AR chromatin interactions are highly plastic and reveal highly consistent programmatic alterations specific to the different stages of prostate cancer [16, 18–21]. As a result of effective AR-inhibiting therapies, metastatic lesions have the potential to display linear plasticity, and aggressive prostate cancer variants may arise, including treatment-emergent neuroendocrine (t-NE) or double-negative (loss of AR and NE markers) prostate cancer [22, 23]. t-NE differentiation is a distinct path of tumor progression in prostate cancer, characterized clinically by low expression of serum PSA and poor survival [24]. Although associated with late-stage disease, the development of t-NE is an early feature of resistance to AR-inhibition and is generally considered an epigenetic phenomenon and defined by transcriptional reprogramming [25, 26]. However, reported genetic traits associated with t-NE include the absence of *AR* amplification, the presence of inactivating mutations in *TP53* and *RB1*, loss of *PTEN*, and amplification of *MYC* in the same sample [25, 27].

Unraveling the genetic determinants underlying metastatic organotropism could contribute to patient stratification for sensitivity to specific therapeutic interventions, improving prostate cancer patient care.

Here, we explored the genetic characteristics associated with the location of prostate cancer metastases, including mutations, amplifications, deletions, and tumor mutational load (TML). Moreover, the mutational patterns in disease stage-specific AR chromatin binding regions were explored and related to functional output. We report on whole genome sequencing (WGS) data from 378 mCRPC biopsies, representing the largest genomic dataset to date in metastatic prostate cancer, as a unique resource for the scientific community, enabling us to evaluate differential genetic traits of metastatic disease with significant power.

Methods

Cohort

The Center for Personalized Cancer Treatment (CPCT) is a nationwide biopsy trial in the Netherlands that collects fresh-frozen biopsies from metastatic sites of all cancers (Additional file 3: CPCT-02 full protocol). Patients with mCRPC were prospectively included in the metastatic site biopsy study between February 2015 and June 2020. Patients included were 18 years or older, had measurable disease according to RECIST 1.1 criteria [28], had metastatic lesions that were safely accessible for a histological biopsy, and were candidates for systemic treatment with a second-generation anti-hormonal therapy (enzalutamide, abiraterone or apalutamide or any other new androgen inhibitor at the discretion of the physician).

The primary outcome of the CPCT-02 study was to evaluate the number of patients with adequate mutational profiling of their cancer genome and multiple secondary outcomes. The primary outcome result in mCRPC patients has been published previously [29].

Adequate biopsy and PBMC germline control WGS was obtained in 69.1% of patients who underwent a metastatic site biopsy.

Samples and genomics features

The Hartwig Medical Foundation (Hartwig) mCRPC cohort contains WGS data from 378 biopsies from unique patients at any stage of metastatic castration-resistant disease, irrespective of (systemic) treatments received. However, all patients received androgen deprivation therapy. For this analysis, we excluded biopsies from the prostate, as these most likely reflect primary tumors. Patients may have had metastases at other sites than biopsied. Biopsies were fresh-frozen in liquid nitrogen, followed by an assessment of tumor cellularity estimated in hematoxylin–eosin-stained 6-µm thick sections. A minimal tumor content of the biopsy of 30% was accepted for further processing (see [29]). WGS data of the biopsies was processed uniformly using the same pipeline. In short, between 50 and 200 ng of DNA were used for sequencing on a HiSeqX (Illumina) sequencer. The resulting reads were mapped to the GRCH37 version of the genome using BWA-MEM. Single nucleotide variants and indels were called using Strelka with optimized settings. Structural variants were called using Manta. A complete workflow description is found elsewhere [30, 31].

Hartwig performed whole genome sequencing (WGS) for 386 metastatic castration-resistant prostate cancer samples, of which 378 were from metastatic sites, categorized as LN, bone, liver, or visceral metastases. Visceral biopsies were defined as any taken from the peritoneal or thoracic cavity except the liver. We excluded biopsies from the prostate as they are too similar to the primary tumor and do not represent metastasis. A clinician manually curated the sample classification.

The genomic data was processed at Hartwig [30]. All samples were processed identically. The analyses were performed using all data unless stated otherwise. For generation of the mutation/copy number and structural variant data, we used the data from the purple analysis pipeline, which is downstream of the primary mutation and variant calling and prioritized genes as likely drivers. Hartwig provided this data. The driver gene list selection method is described in Priestley et al., Supplemental Materials Sect. 21 [30]. The mutational signature and AR chromatin binding site analyses were performed using the whole genome somatic mutation data. The complete definition of the Hartwig pipeline is found here: https://github.com/hartwigmedical/pipeline5.

Genes with at least ten altered samples were considered for downstream analysis. The Hartwig data processing includes patient-matched blood (PBMC) samples, but an exploration of germline data was out of the scope of this analysis.

Genomic regions selectively occupied by AR and altered upon tumorigenesis (gained in tumor (GIT) or lost in tumor (LIT)) or metastasis formation (gained in metastases (GIM) and lost in metastases (LIM)) were reported previously [16, 19, 20].

Clinical data

Apart from the biopsy site as provided in the database, data on the number of organs affected by metastases could be secured separately from a total of 233 patients, of whom 87 (37.3%) had a bone biopsy, 23 (9.9%) had a liver biopsy, 115 (49.4%) had a LN biopsy, and 8 (3.4%) a visceral biopsy. However, no data on the number of metastases or metastatic load was available.

Association of genomic features with biopsy site and tumor mutation burden

Biopsy site

A generalized Fisher exact test was used to determine whether the gene is non-uniformly altered across biopsy sites. Multiple testing corrected p values, using the Benjamini–Hochberg procedure, are designated as p-adjust.

Tumor mutation load

We tested whether genes were associated with the tumor mutation load for each biopsy site, as defined in the previous section. For that purpose, we performed a t-test comparing the tumor mutation load in altered samples against wild-type samples. We corrected the p values for multiple tests using the Benjamini–Hochberg procedure. For a high TML qualification, the Hartwig threshold of > 140 missense mutations was used.

Comparison with primary prostate cancer cohort (TCGA)

We used the TCGA Prostate Adenocarcinoma, as sourced data from GDAC Firehose (https://gdac.broadinstitute.org) by cBioportal (https://www.cbioportal.org). The gene-altered status combines mutation status (comprising putative drivers and VOUS) with copy number alterations by Gistic2. The sample altered status was downloaded directly from the cBioportal.org website and used for the downstream comparative analyses.

Mutational signatures

We used the R package MutationalPatterns (v3.0.1) [32] for inferring mutational (RefSeq) signatures [33].

Neuroendocrine (NE)-potential score

Three genetic traits associated with t-NE were selected to construct a NE-potential score: (1) the absence of AR amplification, (2) the presence of inactivating mutations

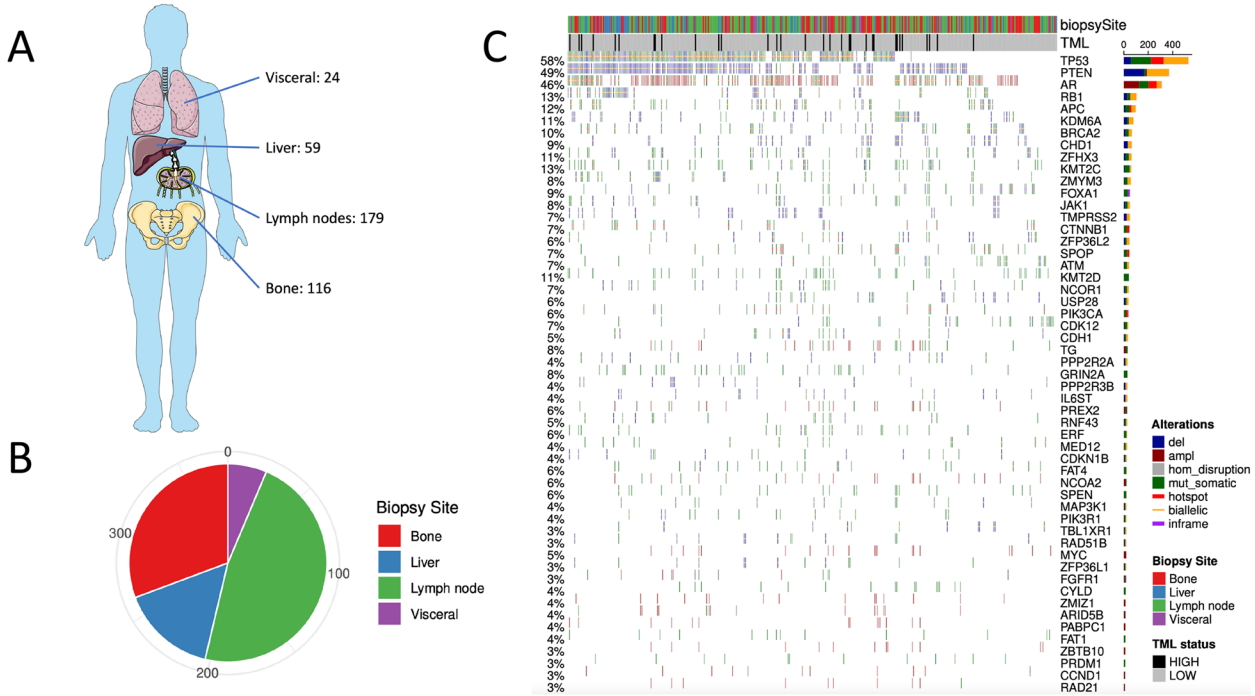

Fig. 1 Origin and genetic characterization of prostate cancer metastatic sites. **A** Overview of the number of biopsy samples collected from each metastatic site (https://smart.servier.com). **B** Distribution of metastatic sites in the dataset. **C** Oncoprint shows this cohort's most frequent mutations and recurrently deleted or amplified genes

of TP53, and (3) the presence of inactivating mutations of RB1 [25, 27]. The score per biopsy site is 0, 1, 2, or 3 genetic traits, of which 3 genetic traits qualify for high NE potential.

Results

Patient cohort characterization

Of the 378 metastatic samples, 179 originated from a LN, 116 from bone, 59 from liver, and 24 from visceral sites (Fig. 1A and B). Visceral samples comprise biopsies taken from any organ in the abdominal or thoracic cavity, apart from the liver, bone, or LN, thus constituting a more heterogeneous group than the other sites (Additional file 1: Table S1). The number of organs affected by metastases was lower at diagnosis than at the time of biopsy (Additional file 2: Fig. S1). At the time of biopsy, patients who had a liver or visceral metastasis biopsy had more metastatic sites than patients with a bone or LN metastasis biopsy (Additional file 2: Fig. S1, Additional file 1: Table S2), which agrees with the occurrence of these metastatic sites in late-stage disease.

We generated an overview of the most common genetic alterations observed in the cohort, affecting at least 10 patients (Fig. 1C). The most common aberrations were *AR* amplifications, followed by deletions or mutations in *RB1*, *TP53*, and *PTEN*. *TMPRSS2-ERG* was the most common gene fusion (Additional file 2: Fig. S2). These findings are consistent with a previously reported analysis of 197 samples from the same cohort [29] and other studies evaluating whole exome sequencing (WES) data [34].

Genomic patterns aligning with neuroendocrine differentiation

Next, we assessed genetic features previously associated with t-NE mCRPC: absence of *AR* amplifications, the occurrence of inactivating mutations of *RB1* and *TP53*, loss of *PTEN*, and amplification of *MYC* [25, 27]. Nearly all *RB1* losses also showed *PTEN* loss, while high *MYC* amplification levels were mutually exclusive from these other genetic traits. Based on these findings, we created an NE-potential score, which is the sum of the occurrence of three genetic traits: inactivating alterations in *TP53* and *RB1* and the absence of *AR* amplification (Additional file 2: Fig. S3). We found 33 (8.7%) patients whose genetic alteration pattern suggested NE-potential (all three features). Interestingly, the biopsy site was strongly associated with NE-potential (generalized Fisher exact, p value: 1.2e−9): 25.0% of the visceral and 27.1% of the liver metastases carried a high NE-potential, while only 5.2% of the bone and 2.8% of the LNs did (Additional file 2: Fig. S4). When we looked more specifically at the

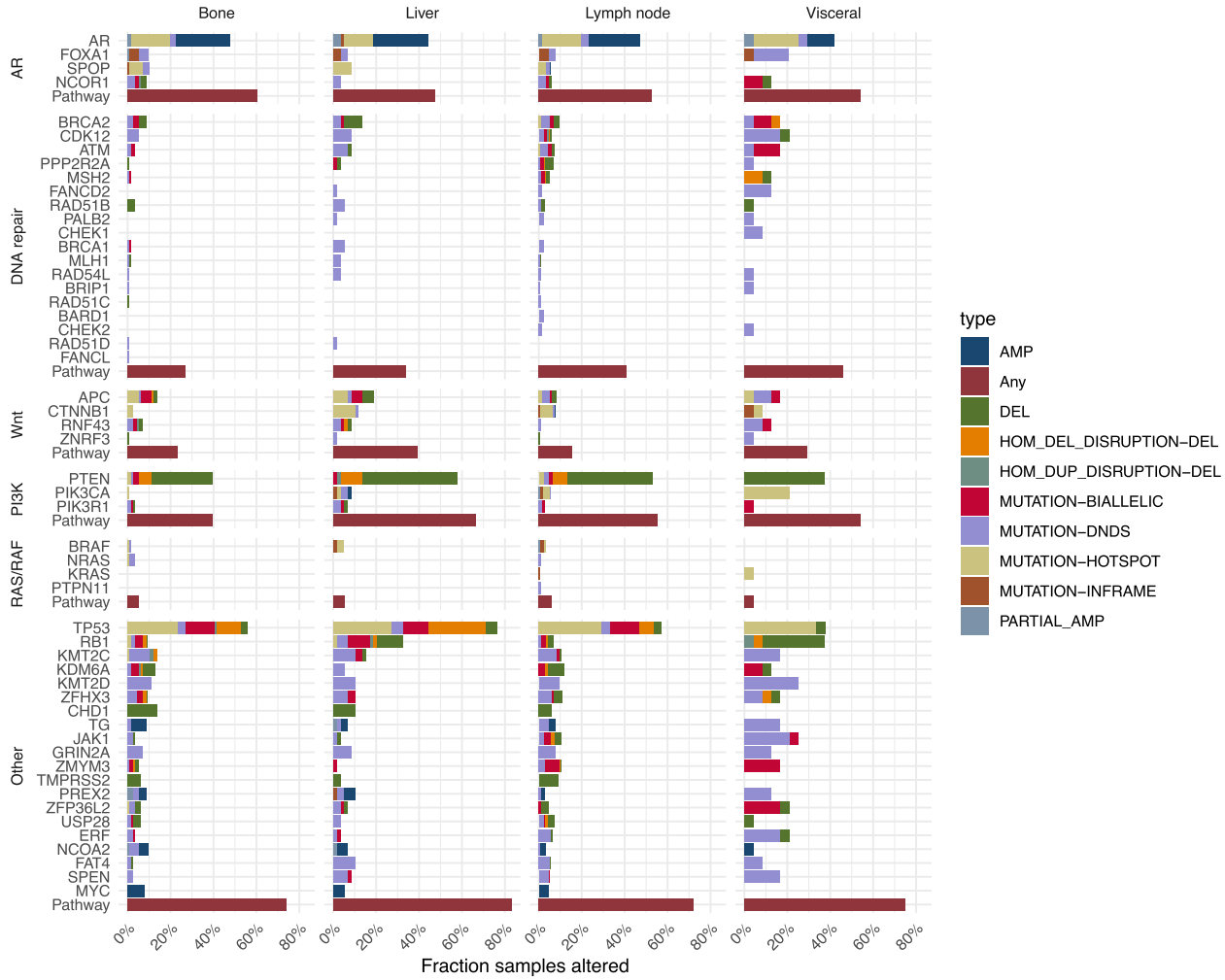

Fig. 2 Frequencies of prostate cancer-relevant gene alterations between metastatic sites. Overview of the alteration frequencies of genes in metastatic sites, clustered by their associated pathway. In addition, the aggregated pathway analysis, based on alteration frequencies within these pathways, is shown for the different sites

number of genetic features that make up the NE-potential score, we saw that one or two alterations in bone and LN metastasis were common, but all three were rarely co-occurring (Additional file 2: Fig. S4). In contrast, we observed one to three alterations in almost equal frequency for liver and visceral metastasis.

The differential mutational landscape between prostate cancer metastatic sites

After identifying the most frequent aberrations and gene fusions in the cohort, we assessed the differential frequencies of amplifications, deletions, and mutations of these commonly mutated genes in mCRPC between metastatic sites. We marked a sample as "altered" when we observed any of these alterations. We reported hotspot mutations when genes carried multiple alterations. Genetic traits were grouped by their associated pathway, while genes not associated with a pathway were collated as "other" (Fig. 2). The complete list of gene alteration counts can be found in Additional file 4: Table S3. We compared gene mutation frequency distributions across different sites using a generalized Fisher exact test and the Benjamini–Hochberg procedure to control for multiple testing [35]. Interestingly, while the alteration frequencies were similar for most genes across the metastatic sites, some reflect a site preference (Additional file 5: Table S4). The differential alteration frequencies between biopsy sites that reached significance were *RB1* (p-adjust: <0.01), *PIK3CA* (p-adjust: 0.03), *JAK1* (p-adjust: 0.03), *RNF43* (p-adjust: 0.03), and *TP53* (p-adjust: 0.05) (Fig. 2). A previous study reported enrichments of MYC amplification, PTEN deletion, and PIK3CB amplifications in liver metastases compared to other metastatic sites [36]. However, we found that alterations in *RB1* occurred more

frequently in liver and visceral metastases, specifically gene deletions ($n=7$, 11.9% and $n=7$, 29.9%, respectively), compared with LN and bone ($n=5$, 2.8% and $n=1$, 0.9%, respectively) (p-adjusted: 0.0002) (Fig. 2). Relatively few *PIK3CA* hotspot mutations were found in bone ($n=1$, 0.9%), liver ($n=1$, 1.7%), and in LN ($n=6$, 3.3%) compared to visceral sites ($n=5$, 21%) (p-adjust: 0.041), suggesting a role of these alterations in metastatic organotropism. However, since liver and visceral biopsies had the highest NE-potential score (Additional file 2: Fig. S3), t-NE differentiation is an alternative explanation for the higher frequency of gene alterations in these sites. Of the gene rearrangements, *TMPRSS2-ERG* fusions were found in 45–50% of bone, liver, and LN samples, while in 38% ($n=9$) of visceral samples (p value: ns) (Additional file 2: Fig. S2). In contrast, *CNTNAP2* and *MACROD2* rearrangements were found in 38% and 33% of visceral samples, respectively, compared to 12–22% and 13–17% in bone, liver, and LN samples. However, these differences in occurrence did not reach significance (p-adjust: 0.18 and 0.28, respectively). While these genes have not been implicated in prostate cancer before, *CNTNAP2* has been reported as over-expressed in metastatic breast cancer, while *MACROD2* is implicated in liver cancer metastasis [37, 38].

The visceral metastases group is heterogeneous (Additional file 1: Table S1), with various impacts of sites on patient prognosis. For instance, lung metastases have a relatively small impact on prognosis [39]. Therefore, comparisons of frequencies of aberrations in sites within the visceral metastases group would have been of added value. However, the number of samples per site was considered too low to make reliable comparisons.

Prostate cancer metastases do not develop simultaneously in the various organs and liver, and visceral metastases are associated with late-stage disease [40]. Therefore, the timing of metastasis development at a particular site may be associated with the accumulation of metastases and frequency of NE potential. Furthermore, only one metastatic site biopsied was considered per patient. Based on the current data, it cannot be excluded that the genetic features of the biopsy can be generalized to other metastatic lesions within the same patient. We clustered the samples into three groups to address these confounding factors: no-bone metastases, no-LN metastases, and no soft-tissue (liver and visceral) metastases. Of all the genes analyzed for mutations listed in the oncoplot, only a higher frequency of *RB1* (p-adjust: 0.0012) was found in patients with soft-tissue metastases, while fewer *PRDM1* (p-adjust: 0.0094) mutations were found in biopsies of patients with bone metastases (Additional file 1: Table S5A and B). *PRDM1*, encoding for the BLIMP1 transcription factor, has been associated with T-cell stemness and exhaustion [41], but no relation with prostate cancer bone metastasis was previously described.

After identifying genetic traits associated with the metastatic process, organotropism, or both, we assessed prostate cancer-relevant pathways for organotropism with emphasis on targetable pathways, including AR signaling, PI3K signaling, WNT signaling, DNA repair, and MAP-kinase pathways [42–46]. The fractions of altered samples (with genomic alterations in the pathway) were compared across the various metastatic sites using a generalized Fisher exact test and the Benjamini–Hochberg procedure to correct for multiple hypothesis testing [35]. WNT pathway alterations (p-adjust: 0.01) were higher in liver metastases than in the other metastatic sites, while PI3K pathway alterations (p-adjust 0.02) were lower in bone than in other sites (Additional file 5: Table S4). Genetic alterations associated with t-NE differentiation may partly explain these findings because of the high NE-potential score of liver and visceral metastases. Additionally, we found a trend for differential mutations of DNA repair genes (p-adjust: 0.12) with relatively few in bone. There were no differential alterations between metastatic sites in the other pathways assessed.

Mutational patterns at disease stage-specific AR chromatin-bound sites and their functional consequences

As a consequence of the high plasticity of AR chromatin interactions, varying with disease stage, prior studies identified consistent and programmatic alterations of AR chromatin profiles in tumorigenesis (coined as GIT or LIT) or metastasis formation (coined as GIM or LIM) [16, 19, 20]. The availability of WGS data allowed us to evaluate the mutation frequency of these regions for the metastatic site. While there was no difference in the mutational frequency of GIT, LIM, and LIT regions between metastatic sites, the GIM regions were more often mutated in bone metastases than other sites (Additional file 2: Fig. S5). At these GIM regions, we found that mutations were predominantly intronic and distal intergenic sites, typical for AR-bound sites [17]. However, between metastatic sites, no difference in the distribution of type of mutations at GIM regions was found (Additional file 2: Fig. S6). Subsequently, we applied gene set enrichment analysis based on the AR site-proximal genes (Additional file 2: Fig. S7). Strikingly, the hallmark UV response, which represents DNA repair, is enriched in all four metastatic sites, suggesting that non-coding mutations at AR-bound sites in metastatic prostate cancer affect genes involved in DNA repair, which seems especially the case for bone metastases.

Comparison of gene alterations between primary prostate cancer and metastatic sites

Following identifying genetic traits with a differential frequency between metastatic sites, we explored differences in gene alteration frequencies between primary prostate cancer and metastatic sites using a two-sided Fisher's exact test and a Benjamin-Hochberg procedure to account for multiple testing. This comparison allowed us to discriminate between gene alterations associated with the metastatic process, organotropism, or both. To this end, we compared the alteration rates in our 378-tumor metastatic cohort with WES data from 492 primary prostate cancers from The Cancer Genome Atlas using cBioPortal (TCGA) [47].

Comparisons of gene aberrations between metachronous same-patient treatment naïve primary prostate cancer samples and mCRPC metastases were made previously in 61 patients [48]. Although our primary and metastatic disease comparisons were not in the same patient, the more considerable statistical power of the greater sample numbers might yield novel insights.

Twelve of the 492 (2.4%) primary prostate cancers fulfilled the NE-potential score criteria, which is lower than the 7.4% we found in the metastatic samples we analyzed. Subsequently, we explored all 61 genes commonly mutated in prostate cancer (see also Fig. 2) for differential alteration frequencies between primary castrate-sensitive prostate cancer (TCGA) and our mCRPC cohort. Of the gene alteration frequencies not different between metastatic sites, alterations in *AR* are uncommon in primary disease ($n=9$, 2%) but widespread in metastatic disease ($n=175$, 46%) (p-adjust <0.001), as expected and extensively described previously [49]. Also, for *PPP2R3B* and *FAT1* alterations, we observed a similar enrichment between the various metastatic sites, suggesting no role in metastatic organotropism. However, the elevated frequency of alterations in these genes for the metastatic samples (log2-fold change of 1.97 and 1.87, respectively) suggests a link with the metastatic process. We also found genes more frequently altered in the primary samples than in the metastatic samples, suggesting that these variants and indel alterations are associated with less metastatic potential. These genes include *PRDM1*, *PPP2R2A*, *FGFR1*, *TMPRSS2*, and *RAD21*, of which *TMPRSS2* is the most commonly altered gene and found in 7% ($n=25$) of the metastatic samples and 16% ($n=80$) of the primary samples (p-adjust <0.001). Although there is much research into *TMPRSS2-ERG* fusions [50], there are, to our knowledge, no reports on the role of point mutations in *TMPRSS2* in prostate cancer development.

Of the five genes which showed organotropism, *RB1*, *PIK3CA*, *JAK1*, *RNF43*, and *TP53* (Additional file 5: Table S4), we found enrichment only for *TP53* alterations in mCRPC ($n=221$, 58%) compared with primary disease ($n=88$, 18%) (p-adjust <0.001), which might suggest a role of functional *TP53* loss in the metastatic process. The remaining four genes had comparable frequencies in primary cancer and metastases, suggesting that alterations in these genes confer no general propensity to the metastatic process. Samples with *RB1* alterations were found in equal frequencies in primary ($n=83$, 17%) and mCRPC samples ($n=51$, 13%). Although less frequent, we observed similar tendencies for the other gene alterations that showed organotropism with a penchant for visceral sites, *PIK3CA*, *JAK1*, and *RNF43*, which are relatively rare in primary and metastatic disease (<7% in both compartments). Of note is that the differences in mutation frequencies between primary and metastatic disease might reflect the time of development and tumor evolution, as primary disease precedes metastatic cancer.

Tumor mutational load and mismatch repair deficiency are most pronounced in liver and visceral metastases

Finally, we explored broad characteristics of DNA aberrations, such as the type of aberration, tumor mutational load (TML), and mutational signatures. TML is the total number of somatic missense variants across the whole genome of the tumor [31, 51]. Metastases to the liver and visceral sites showed the highest TML (Fig. 3A). A comparison of the mean TML across biopsy sites showed more missense mutations, the defining feature of TML, in the liver (mean: 131, IQR 42–70) and visceral metastases (mean: 290, IQR 50–86) as compared to bone (mean: 59, IQR 36–58) and LN samples (mean: 96, IQR 36–71) (ANOVA, $p<0.001$) (Fig. 3B). The mutational process frequently leaves traces known as mutational signatures, allowing for its identification [52]. We queried the *Signal Reference* signatures (Ref.Sig.) [33] for all samples from all metastatic sites (Additional file 2: Fig. S8). We observed a high burden of Ref.Sig. 1 mutational signature. This signature is known to be associated with age, which might be expected because prostate cancer mainly affects older men. More importantly, we found a cluster with a high score for Ref.Sig.MMR1 and Ref.Sig.MMR2, both associated with defective mismatch repair (MMR). Other reference signatures were Ref.Sig. 18 and 17, both of unknown etiology [33]. Nine cases with high-TML unexplained by MMR signatures were associated with high Ref.Sig. 8, and Ref.Sig.3 fractions, but not 5 (Additional file 2: Fig. S9). Ref.Sig.8 tends to cluster with Sig.3 and Sig.5 [33] and is associated with homologous repair deficiency. While Sig.8 is of unknown etiology, Sig.3 is implicated in BRCA1/2 germline/somatic mutations [33], and indeed, mutation data confirmed BRCA2 mutations or deletions in six patients. Ref.Sig.5 is associated with smoking, and this may explain the low contribution.

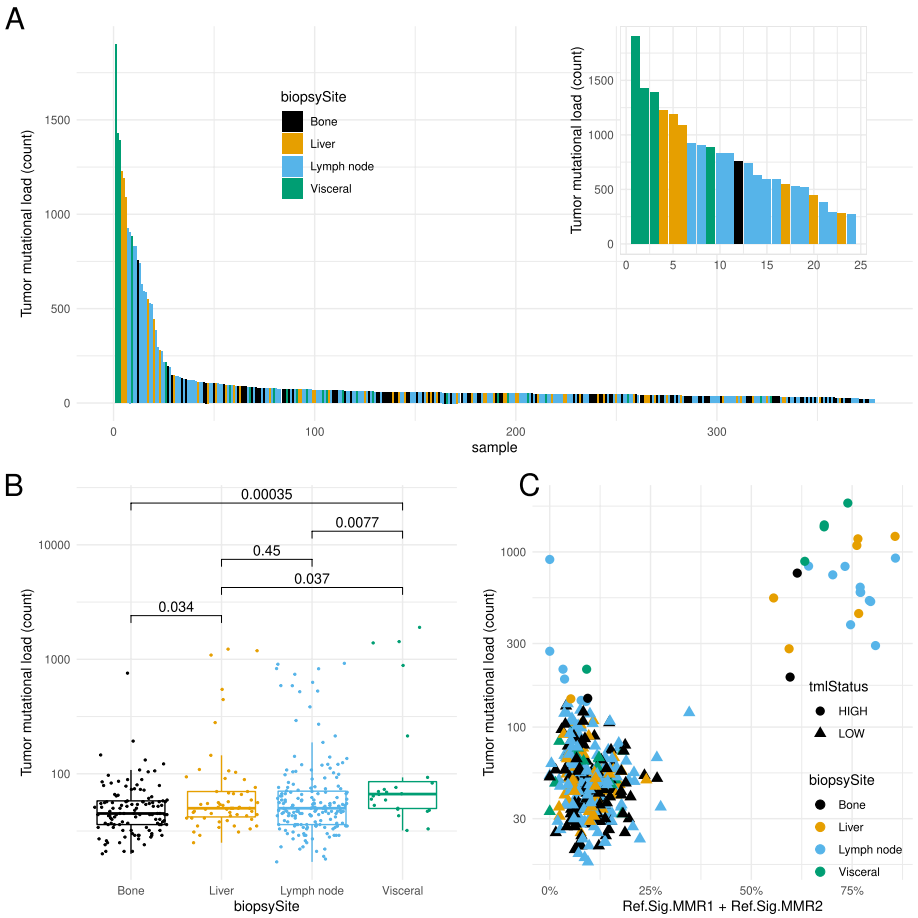

Fig. 3 TML by metastatic sites in relation to MMR deficiency. **A** Waterfall plot of TML in all samples. Y-axis: number of missense mutations. The insert shows the 25 samples with the highest TML. **B** Boxplot showing the TML per biopsy site (*p* value by *t*-test). **C** Dotplot showing the fraction of mutations explained by Ref.Sig. MMR1 and MMR2 (no dimension; x-axis) and their relation with TML (mutations per megabase; y-axis, log scale). High-TML is defined as > 140 missense mutations

Next, we explored the relationship between TML and MMR signatures (Fig. 3C) and found that most high-TML samples [30, 31] had more than 50% of the missense mutations explained by the MMR signature (Fig. 3C). The frequency of high TML showed organotropism and was predominantly determined by Ref.Sig.MMR1 (Additional file 2: Fig. S10). Most high-TML cases are also microsatellite instable (MSI)-high, and the MSI status is one explanation for the large number of point mutations. Interestingly, none of the samples recognized as MSI-high had a high NE potential, suggesting MSI-high as an orthogonal group not associated with t-NSE differentiation (Additional file 2: Fig. S3). MSI-high tumors exhibit more aggressive biology, which may be associated with more extensive disease [53]. Although no exact information on the metastatic load of patients in the cohort was available, we used the number of organs affected with metastases as a proxy for the metastatic volume. No relation was found between TML and the number of metastases affected organs in all four biopsy site groups (Additional file 2: Fig. S11).

Subsequently, we used the Hartwig driver assessment (see Methods) to test whether the mutational status of the DNA repair genes was associated with TML relative to the site of metastasis. A positive relation between DNA-repair-associated gene alteration state and TML was expected, but this does not have to be true for all gene-site combinations. Of the homologous recombination DNA-repair-associated genes, *BRCA2* mutations were associated with a higher TML in all biopsy sites, while *ATM* and *FANCD2* were associated with a higher TML in visceral samples only (FDR < 0.2). Also, mutations in the epigenetic modifiers previously described to be involved in DNA damage response *KMT2C* and *KMT2D* [54, 55] were associated with a higher TML in liver, visceral, and LN samples (FDR < 0.2), while *ZMYM3* [56] was only associated with a higher TML in visceral samples. *MSH2* mutations were associated with a higher

TML in all sites, no *MSH2* mutations were found in liver samples (Additional file 2: Fig. S12), and TML was higher in liver and LN samples with *MLH1* mutations. Similarly, JAK1 mutations showed a trend (p-adjust: 0.06) for TML association in visceral metastases. Generally, *MSH2* driver alterations are rare (1%) in primary prostate cases (TCGA) but are more frequent (4%) in metastatic patients (this cohort) [47]. A non-significant (p-adjust 0.136) trend for a higher incidence of *MSH2* alterations was found in visceral samples (13%), as compared to bone (2%), liver (0%), and LN (4%) samples (Additional file 5: Table S4). Alteration rates for *MLH1* were relatively low, with 2% and 1% in metastatic and primary samples, respectively, without clear evidence of organotropism (Additional file 5: Table S4).

In conclusion, we identified distinct mutational profiles between metastatic sites with possible therapeutic implications by analyzing the largest WGS dataset on metastatic prostate cancer generated to date.

Discussion

Metastatic dissemination is the process by which cancer cells spread from their primary location to other organs in the body [9]. Different types of cancer tend to spread to specific organs, which suggests that germline and somatic mutations may play a significant role in the dissemination process [9]. However, it is unclear how the genetic traits of prostate cancer cells enable them to spread to specific tissues or how tumors develop genetic alterations at the site of metastasis.

Commonly clinically applied panel sequencing has limited resolution to assess molecular events since it only probes a small part of the genome [57]. To identify the genetic characteristics of metastatic prostate cancer, we therefore used the largest WGS dataset generated to date on mCRPC samples. Samples with a high NE potential, suggesting t-NE differentiation, were rare in bone and LN samples but more frequent in liver and visceral samples, which has been described previously [24]. We found that alteration frequencies across metastatic sites were similar for most genes, but some mutations were site-specific. *RB1*, *PIK3CA*, *JAK1*, *RNF43*, and *TP53* were the most frequently altered genes, with *RB1*, *PIK3CA*, and *TP53* already known to be drivers of prostate cancer development [58]. Although suggestive of a role in organotropism, genetic traits with a higher frequency in liver and visceral samples might also be explained by differential clonal selection due to multiple treatments and the development of t-NE differentiation between metastatic sites.

We evaluated the mutation frequency of clinically relevant AR chromatin binding sites and found a higher frequency of mutations in bone compared to the other metastatic sites only in the GIM regions. Gene set enrichment analysis identified DNA repair mechanisms as the most significantly enriched process for those mutated AR sites, suggesting that non-coding mutations converge on this biological process in metastatic disease. This interesting observation warrants deeper functional biological exploration in follow-up studies.

Surprisingly, only *TP53* mutations showed a higher frequency in mCRPC metastases than in primary prostate cancer, which suggests that *RB1* and *PIK3CA* are not required for cells to metastasize, but *TP53* mutation potentially is. A previous study of paired biopsies of primary prostate cancer and mCRPC metastases of 61 patients reported an increase of *AR* mutations and amplifications, as well as an increase of *TP53*, *RB1*, and *PI3K/AKT* mutations in metastatic sites [48], confirming our finding of higher *TP53* mutation frequencies in metastases. Mutations of the WNT-pathway-associated *RNF34* gene are associated with resistance of mCRPC to AR-targeted therapies [59]. *JAK1* and *RNF43* alterations can be considered passenger mutations, and no difference in the occurrence between primary disease and mCRPC metastases [58] was observed. In turn, for *PPP2R3B* and *FAT1* alterations, we observed an enrichment in the metastatic setting but no selectivity for particular metastatic sites. *PPP2R3B* is a subunit of protein phosphatase 2A, and alterations have been associated with poor prognosis of metastatic melanoma but have not been studied in mCRPC, while *FAT1* was identified as a tumor suppressor in prostate cancer cells [60, 61]. Therefore, alterations of *PPP2R3B* and *FAT1* might contribute to an aggressive phenotype.

We observed a higher TML in liver and visceral metastases than in bone and LN metastases. Surprisingly, a high TML was mutually exclusive with a high NE potential, suggesting two parallel tracks of prostate cancer progression in the advanced disease setting, with high TML precluding neuroendocrine differentiation. Over half of the mutations in the samples with high TML could be explained by a DNA mismatch repair (MMR)-deficiency mutational signature. MMR deficiency increases the likelihood of acquiring somatic mutations, particularly in short repetitive sequences, leading to varying lengths of these regions, termed microsatellite instability (MSI) [62]. MMR signatures could not explain some of the high TML samples, and deeper investigation into the mutational signatures pointed to homologous repair deficiency associated with loss of BRCA1/2, which was corroborated by 6 out of 9 samples indeed presented with BRCA1/2 mutations—the functional role of Ref.Sig. 8, which significantly contributed to our observed mutations, is unknown. Ref.Sig. 3 is associated with BRCA1/2 loss of function, but the clustering of these two signatures

is consistent with previous findings, possibly hinting at a complex interplay between the mechanisms underlying these signatures [33]. In the current cohort, a trend towards organotropism was found for mutations of the MMR-associated gene *MSH2*, with relatively high rates in visceral samples. Another driver gene alteration associated with a higher TML in visceral metastases was *JAK1*. While *SPEN* and *PREX2* are not reported to be associated with DNA repair mechanisms, *JAK1* loss of function is associated with MSI in multiple cancers, including prostate cancer [63]. It is suggested that *JAK1* loss of function alterations represent an adaptation to immune responses against MSI tumors and contribute to tumor immune evasion through an interferon response [63].

Few studies have reported on molecular organotropism of prostate cancer previously. A large pan-cancer cohort identified associations between genomic alterations and patterns of metastatic dissemination [34], in which genomic characterization was performed by targeted sequencing of a panel of 341–468 cancer-associated genes. This study included targeted panel sequencing of 860 metastatic prostate cancer samples (no WGS), revealing a slight increase in mutation frequency observed in liver metastases without differential TML between metastatic sites. Liver metastases were associated with increased *PTEN* deletion, *MYC* amplification, and increased *PI3K* and *MYC* signaling, while bone metastases were associated with decreased representation of *ERG* fusions and lung metastases displaying fewer *AR* amplifications [34]. These results agree with our current findings on increased *PTEN* deletion and elevated *PI3K* signaling in liver metastases, but we did not find increased *MYC* amplification in liver metastases or a higher frequency of *ERG* fusions in bone metastases compared to other sites.

However, we established differential alterations of more genes between metastatic sites and increased TML in liver and visceral metastases. Some discrepancies might be related to differences in techniques, as WGS can discover biologically and clinically relevant signals comprehensively and unbiasedly that are often missed by the limited gene panel of targeted sequencing. Furthermore, panel sequencing has been reported to have limited resolution in establishing genetic relations [57].

Metastatic organotropism has also been studied in other cancer types, including breast cancer [64]. Although prostate cancer and breast cancer are hormone-dependent and share multiple molecular features [65], the genetic traits driving metastatic site selection share surprisingly little overlap between the cancer types. This lack of overlap suggests that the molecular component of metastatic site preference of prostate and breast cancer follows different routes.

High-TML incidence varies markedly across tumor types [66] and is common in canonical mutagen-associated cancers, including skin (ultraviolet light) and lung (tobacco smoke) [52]. Consequently, approximately half of melanoma and non-small cell lung cancers (NSCLC) meet the criteria for high-TML [66]. In contrast, less than 5% of prostate cancers have been reported as high-TML [67]. Tumors with high-TML produce many neoantigens that lead to increased tumor immunogenicity, rendering tumors more susceptible to immunotherapeutics [68]. Several studies have demonstrated an association between high-TML and the response of melanoma and NSCLC to immunotherapeutics [69]. Multiple randomized trials showed limited immunotherapeutic efficacy in treating unselected patients with mCRPC [70–72]. In the present study, we report a higher TML in prostate cancer metastases in the liver compared to other metastatic sites. While compelling, claims on the response of these metastases to immunotherapy cannot be made, as no clinical trials to date have evaluated the efficacy of immunotherapy in patients with specific organ metastases. Some circumstantial support can be derived from the results of the KEYNOTE-921 trial, in which mCRPC patients were randomized between docetaxel and docetaxel in combination with pembrolizumab, a monoclonal antibody inhibiting programmed cell death protein-1 [72]. Although no radiographic progression-free survival or overall survival benefit was established in the whole population, the 67 patients in the trial with liver metastases tended to have better radiographic progression-free survival than patients with other metastatic sites (HR 0.61 (0.35–1.08)), suggesting that mCRPC metastases in the liver could be more sensitive to immunotherapeutics than other metastatic sites.

Our study has several limitations. Although genetic traits accumulate over time and are selected by emerging resistance to previous treatments, we do not present the timing or evolution of the WGS biopsies. Moreover, the biopsy site was not predefined, and no patient received multiple biopsies simultaneously. Therefore, it cannot be excluded that metastatic sites in the same patient harbor different mutations. The large number of samples partly overcomes this uncertainty. Another limitation is the absence of information on treatments and treatment outcomes. Therefore, the present study cannot evaluate a relation between high TML metastases and response to immunotherapy and between other genetic aberrations and targeted therapy. Finally, the constructed NE-potential score represents a likelihood of an NE phenotype, but pathology evaluations and immunohistochemistry are required to identify such an NE phenotype conclusively.

Conclusions

In summary, *RB1*, *PIK3CA*, *JAK1*, *RNF43*, and *TP53* mutations were identified as the most frequent genetic determinants associated with site selectivity for prostate cancer metastatic outgrowth. We found that frequencies of mutations of metastatic disease-specific AR chromatin binding sites were higher in bone metastases and converged on pathways that impact DNA repair. These results suggest a critical role of mutations in the non-coding genome in prostate cancer metastatic outgrowth and/or tumor progression. Furthermore, liver and visceral metastases had a higher TML than bone and LN metastases, which were strongly associated with DNA mismatch repair (MMR)-deficiency features. Based on these observations, we hypothesize that patients with metastases that are found predominantly at sites associated with high-TML (namely liver and visceral) are more likely to respond to immunotherapeutics treatment based on relations between TML and immunotherapy response, as established in other cancer types. Therefore, preselecting mCRPC patients based on metastatic sites could prove a critical step in future clinical trial design.

Abbreviations

AR	Androgen receptor
CPCT-02	Center for Personalized Cancer Treatment, study-02
GDAC	Genome Data Analysis Center (Broad Institute)
GIM	Gained in metastases
GIT	Gained in tumor
LIM	Lost in metastases
LIT	Lost in tumor
LN	Lymph node
mCRPC	Metastatic castration-resistant prostate cancer
MMR	Mismatch repair
MSI	Microsatellite instability
NE-potential score	Neuroendocrine potential score
NSCLC	Non-small cell lung cancer
PBMC	Peripheral blood mononuclear cell
RECIST 1.1	Response Evaluation Criteria in Solid Tumors, version 1.1
Ref.Sig.	Signal Reference signature
TCGA	The Cancer Genome Atlas
TML	Tumor mutational load
t-NE	Treatment-emergent neuroendocrine
UV	Ultraviolet light
VOUS	Variants of unknown significance
WES	Whole exome sequencing
WGS	Whole genome sequencing

Supplementary Information

The online version contains supplementary material available at https://doi.org/10.1186/s13073-025-01445-5.

Additional file 1. Contains supplementary tables S1, S2, and S5

Additional file 2. Contains supplementary figures S1–S12

Additional file 3. Contains CPCT-02 full protocol

Additional file 4. Contains Table S3

Additional file 5. Contains Table S4

Acknowledgements

This publication and the underlying study have been made possible based on the data that the Hartwig Medical Foundation and the Center of Personalised Cancer Treatment (CPCT) have made available for the study (HMF-DR-249). We thank René Bernards (NKI, Amsterdam) for the critical reading of the manuscript, Tesa Severson for performing the AR-binding site analyses, the NKI RHPC facility for providing computational resources, and the patients who donated a biopsy to the CPCT for scientific research.

Authors' contributions

Conceptualization: D.V., M.S.H., W.Z., A.M.B.; resources: N.M., M.P.L., E.C., M.S.H., A.M.B.; data analysis: D.V., M.C., L.F.A.W.; writing (initial draft): S.A.L.P.; writing (review and editing): D.V., E.C., N.M., M.P.L., M.S.H., W.Z., A.M.B. All authors read and approved the final manuscript.

Funding

This study was supported by a KWF-Alpe d'HuZes Grant (NKI 2014–7080) and other sources.

Data availability

The data supporting this study's findings are available from Hartwig Medical Foundation, licensed under data request number DR-249. Both WGS and clinical data from the Hartwig Medical Foundation are freely available for academic use through standardized procedures. Patient-level genome-wide germline and somatic data (raw BAM files and annotated variant call data) are considered privacy sensitive and available exclusively through an access-controlled mechanism. Data request forms can be found at https://www.hartwigmedicalfoundation.nl (30). Data on the site of metastases of patients in the WGS cohort was collected and made available separately with permission from the National Central Committee on Research Involving Human Subjects, file 2018–4930.

Declarations

Ethics approval and consent to participate

Patients with metastatic disease, including prostate cancer, were included in the CPCT-02 (NCT01855477) metastatic site biopsy study, which was approved by the Medical Ethical Committee of the University Medical Center Utrecht, the Netherlands and was conducted following the Declaration of Helsinki. All patients explicitly consented to WGS and data sharing for cancer research purposes. WGS and clinical data, including primary tumor type and biopsy location, were collected in electronic case record forms and stored in a central database by Hartwig.

Consent for publication

Not applicable.

Competing interests

None of the authors declared any competing interests.

Author details

[1]Division of Molecular Carcinogenesis, Netherlands Cancer Institute, Amsterdam, The Netherlands. [2]Division of Computational Cancer Biology, Netherlands Cancer Institute, Amsterdam, The Netherlands. [3]Center for Molecular Medicine, University Medical Center Utrecht, Utrecht, The Netherlands. [4]Hartwig Medical Foundation, Amsterdam, The Netherlands. [5]Oncode Institute, Utrecht, The Netherlands. [6]Department of Medical Oncology, Radboud University Nijmegen Medical Center, Nijmegen, The Netherlands. [7]Department of Medical Oncology, Erasmus MC Cancer Institute, Erasmus University Medical Center Rotterdam, Rotterdam, The Netherlands. [8]Department of Medical Oncology, Netherlands Cancer Institute, Amsterdam, The Netherlands. [9]Division of Oncogenomics, Oncode Institute, Netherlands Cancer Institute, Amsterdam, The Netherlands.

Received: 17 May 2024 Accepted: 17 February 2025
Published online: 20 March 2025

References

1. Bray F, Ferlay J, Soerjomataram I, Siegel RL, Torre LA, Jemal A. Global cancer statistics 2018: GLOBOCAN estimates of incidence and mortality worldwide for 36 cancers in 185 countries. CA Cancer J Clin. 2018;68(6):394–424.
2. DeSantis CE, Lin CC, Mariotto AB, Siegel RL, Stein KD, Kramer JL, et al. Cancer treatment and survivorship statistics, 2014. CA Cancer J Clin. 2014;64(4):252–71.
3. Pascale M, Azinwi CN, Marongiu B, Pesce G, Stoffel F, Roggero E. The outcome of prostate cancer patients treated with curative intent strongly depends on survival after metastatic progression. BMC Cancer. 2017;17(1):651.
4. Ahmad K. New progress in treatment of hormone-refractory prostate cancer. Lancet Oncol. 2004;5(12):706.
5. Bubendorf L, Schopfer A, Wagner U, Sauter G, Moch H, Willi N, et al. Metastatic patterns of prostate cancer: an autopsy study of 1,589 patients. Hum Pathol. 2000;31(5):578–83.
6. Gandaglia G, Karakiewicz PI, Briganti A, Passoni NM, Schiffmann J, Trudeau V, et al. Impact of the site of metastases on survival in patients with metastatic prostate cancer. Eur Urol. 2015;68(2):325–34.
7. Drake CG. Visceral metastases and prostate cancer treatment: 'die hard', 'tough neighborhoods', or 'evil humors'? Oncology (Williston Park). 2014;28(11):974–80.
8. Kase AM, Copland JA 3rd, Zhai Q, Tan W. Complete response in patients with lung-only metastatic prostate cancer: outcome analysis. Clin Genitourin Cancer. 2022;20(6):e485–9.
9. Gao Y, Bado I, Wang H, Zhang W, Rosen JM, Zhang XH. Metastasis organotropism: redefining the congenial soil. Dev Cell. 2019;49(3):375–91.
10. Liu Y, Cao X. Characteristics and significance of the pre-metastatic niche. Cancer Cell. 2016;30(5):668–81.
11. Pani G, Galeotti T, Chiarugi P. Metastasis: cancer cell's escape from oxidative stress. Cancer Metastasis Rev. 2010;29(2):351–78.
12. Peinado H, Lavotshkin S, Lyden D. The secreted factors responsible for pre-metastatic niche formation: old sayings and new thoughts. Semin Cancer Biol. 2011;21(2):139–46.
13. Weber GF. Metabolism in cancer metastasis. Int J Cancer. 2016;138(9):2061–6.
14. Barbieri CE, Bangma CH, Bjartell A, Catto JW, Culig Z, Gronberg H, et al. The mutational landscape of prostate cancer. Eur Urol. 2013;64(4):567–76.
15. Gundem G, Van Loo P, Kremeyer B, Alexandrov LB, Tubio JMC, Papaemmanuil E, et al. The evolutionary history of lethal metastatic prostate cancer. Nature. 2015;520(7547):353–7.
16. Pomerantz MM, Li F, Takeda DY, Lenci R, Chonkar A, Chabot M, et al. The androgen receptor cistrome is extensively reprogrammed in human prostate tumorigenesis. Nat Genet. 2015;47(11):1346–51.
17. Stelloo S, Nevedomskaya E, Kim Y, Schuurman K, Valle-Encinas E, Lobo J, et al. Integrative epigenetic taxonomy of primary prostate cancer. Nat Commun. 2018;9(1):4900.
18. Mazrooei P, Kron KJ, Zhu Y, Zhou S, Grillo G, Mehdi T, et al. Cistrome partitioning reveals convergence of somatic mutations and risk variants on master transcription regulators in primary prostate tumors. Cancer Cell. 2019;36(6):674-89 e6.
19. Pomerantz MM, Qiu X, Zhu Y, Takeda DY, Pan W, Baca SC, et al. Prostate cancer reactivates developmental epigenomic programs during metastatic progression. Nat Genet. 2020;52(8):790–9.
20. Severson T, Qiu X, Alshalalfa M, Sjostrom M, Quigley D, Bergman A, et al. Androgen receptor reprogramming demarcates prognostic, context-dependent gene sets in primary and metastatic prostate cancer. Clin Epigenetics. 2022;14(1):60.
21. Stelloo S, Nevedomskaya E, van der Poel HG, de Jong J, van Leenders GJ, Jenster G, et al. Androgen receptor profiling predicts prostate cancer outcome. EMBO Mol Med. 2015;7(11):1450–64.
22. Beltran H, Rickman DS, Park K, Chae SS, Sboner A, MacDonald TY, et al. Molecular characterization of neuroendocrine prostate cancer and identification of new drug targets. Cancer Discov. 2011;1(6):487–95.
23. Berchuck JE, Viscuse PV, Beltran H, Aparicio A. Clinical considerations for the management of androgen indifferent prostate cancer. Prostate Cancer Prostatic Dis. 2021;24(3):623–37.
24. Conteduca V, Oromendia C, Eng KW, Bareja R, Sigouros M, Molina A, et al. Clinical features of neuroendocrine prostate cancer. Eur J Cancer. 2019;121:7–18.
25. Beltran H, Prandi D, Mosquera JM, Benelli M, Puca L, Cyrta J, et al. Divergent clonal evolution of castration-resistant neuroendocrine prostate cancer. Nat Med. 2016;22(3):298–305.
26. Linder S, Hoogstraat M, Stelloo S, Eickhoff N, Schuurman K, de Barros H, et al. Drug-induced epigenomic plasticity reprograms circadian rhythm regulation to drive prostate cancer toward androgen independence. Cancer Discov. 2022;12(9):2074–97.
27. Lundberg A, Zhang M, Aggarwal R, Li H, Zhang L, Foye A, et al. The genomic and epigenomic landscape of double-negative metastatic prostate cancer. Cancer Res. 2023;83(16):2763–74.
28. Eisenhauer EA, Therasse P, Bogaerts J, Schwartz LH, Sargent D, Ford R, et al. New response evaluation criteria in solid tumours: revised RECIST guideline (version 1.1). Eur J Cancer. 2009;45(2):228–47.
29. van Dessel LF, van Riet J, Smits M, Zhu Y, Hamberg P, van der Heijden MS, et al. The genomic landscape of metastatic castration-resistant prostate cancers reveals multiple distinct genotypes with potential clinical impact. Nat Commun. 2019;10(1):5251.
30. Priestley P, Baber J, Lolkema MP, Steeghs N, de Bruijn E, Shale C, et al. Pan-cancer whole-genome analyses of metastatic solid tumours. Nature. 2019;575(7781):210–6.
31. Roepman P, de Bruijn E, van Lieshout S, Schoenmaker L, Boelens MC, Dubbink HJ, et al. Clinical validation of whole genome sequencing for cancer diagnostics. J Mol Diagn. 2021;23(7):816–33.
32. Blokzijl F, Janssen R, van Boxtel R, Cuppen E. MutationalPatterns: comprehensive genome-wide analysis of mutational processes. Genome Med. 2018;10(1):33.
33. Degasperi A, Amarante TD, Czarnecki J, Shooter S, Zou X, Glodzik D, et al. A practical framework and online tool for mutational signature analyses show inter-tissue variation and driver dependencies. Nat Cancer. 2020;1(2):249–63.
34. Nguyen B, Fong C, Luthra A, Smith SA, DiNatale RG, Nandakumar S, et al. Genomic characterization of metastatic patterns from prospective clinical sequencing of 25,000 patients. Cell. 2022;185(3):563-75 e11.
35. Benjamini YH, Y. Controlling the false discovery rate: a practical and powerful approach to multiple testing. JR Statist Soc. 1995:57(1):289–300.
36. Alshalalfa M, Seldon C, Franco I, Vince R, Carmona R, Punnen S, et al. Clinicogenomic characterization of prostate cancer liver metastases. Prostate Cancer Prostatic Dis. 2022;25(2):366–9.
37. Gao R, Pratt CP, Yoon S, Martin-de-Saavedra MD, Forrest MP, Penzes P. CNTNAP2 is targeted to endosomes by the polarity protein PAR3. Eur J Neurosci. 2020;51(4):1074–86.
38. Zhou ZJ, Luo CB, Xin HY, Hu ZQ, Zhu GQ, Li J, et al. MACROD2 deficiency promotes hepatocellular carcinoma growth and metastasis by activating GSK-3beta/beta-catenin signaling. NPJ Genom Med. 2020;5:15.
39. Nakamachi H, Suzuki H, Akakura K, Imamoto T, Ueda T, Ishihara M, et al. Clinical significance of pulmonary metastases in stage D2 prostate cancer patients. Prostate Cancer Prostatic Dis. 2002;5(2):159–63.
40. Pezaro C, Omlin A, Lorente D, Rodrigues DN, Ferraldeschi R, Bianchini D, et al. Visceral disease in castration-resistant prostate cancer. Eur Urol. 2014;65(2):270–3.
41. Jung IY, Narayan V, McDonald S, Rech AJ, Bartoszek R, Hong G, et al. BLIMP1 and NR4A3 transcription factors reciprocally regulate antitumor CAR T cell stemness and exhaustion. Sci Transl Med. 2022;14(670):eabn7336.
42. Augello MA, Den RB, Knudsen KE. AR function in promoting metastatic prostate cancer. Cancer Metastasis Rev. 2014;33(2–3):399–411.
43. Carver BS, Chapinski C, Wongvipat J, Hieronymus H, Chen Y, Chandarlapaty S, et al. Reciprocal feedback regulation of PI3K and androgen receptor signaling in PTEN-deficient prostate cancer. Cancer Cell. 2011;19(5):575–86.
44. Schiewer MJ, Knudsen KE. DNA damage response in prostate cancer. Cold Spring Harb Perspect Med. 2019;9(1):a030486.
45. Taylor BS, Schultz N, Hieronymus H, Gopalan A, Xiao Y, Carver BS, et al. Integrative genomic profiling of human prostate cancer. Cancer Cell. 2010;18(1):11–22.
46. Yeh Y, Guo Q, Connelly Z, Cheng S, Yang S, Prieto-Dominguez N, et al. Wnt/beta-catenin signaling and prostate cancer therapy resistance. Adv Exp Med Biol. 2019;1210:351–78.
47. Cancer Genome Atlas Research N. The molecular taxonomy of primary prostate cancer. Cell. 2015:163(4):1011–25.

48. Mateo J, Seed G, Bertan C, Rescigno P, Dolling D, Figueiredo I, et al. Genomics of lethal prostate cancer at diagnosis and castration resistance. J Clin Invest. 2020;130(4):1743–51.
49. Shiota M, Akamatsu S, Tsukahara S, Nagakawa S, Matsumoto T, Eto M. Androgen receptor mutations for precision medicine in prostate cancer. Endocr Relat Cancer. 2022;29(10):R143–55.
50. Khosh Kish E, Choudhry M, Gamallat Y, Buharideen SM, D D, Bismar TA. The expression of proto-oncogene ETS-related gene (ERG) plays a central role in the oncogenic mechanism involved in the development and progression of prostate cancer. Int J Mol Sci. 2022;23(9):4772.
51. Sha D, Jin Z, Budczies J, Kluck K, Stenzinger A, Sinicrope FA. Tumor mutational burden as a predictive biomarker in solid tumors. Cancer Discov. 2020;10(12):1808–25.
52. Alexandrov LB, Nik-Zainal S, Wedge DC, Aparicio SA, Behjati S, Biankin AV, et al. Signatures of mutational processes in human cancer. Nature. 2013;500(7463):415–21.
53. Nava Rodrigues D, Rescigno P, Liu D, Yuan W, Carreira S, Lambros MB, et al. Immunogenomic analyses associate immunological alterations with mismatch repair defects in prostate cancer. J Clin Invest. 2018;128(10):4441–53.
54. Chang A, Liu L, Ashby JM, Wu D, Chen Y, O'Neill SS, et al. Recruitment of KMT2C/MLL3 to DNA damage sites mediates DNA damage responses and regulates PARP inhibitor sensitivity in cancer. Cancer Res. 2021;81(12):3358–73.
55. Rampias T, Karagiannis D, Avgeris M, Polyzos A, Kokkalis A, Kanaki Z, et al. The lysine-specific methyltransferase KMT2C/MLL3 regulates DNA repair components in cancer. EMBO Rep. 2019;20(3):e46821.
56. Leung JW, Makharashvili N, Agarwal P, Chiu LY, Pourpre R, Cammarata MB, et al. ZMYM3 regulates BRCA1 localization at damaged chromatin to promote DNA repair. Genes Dev. 2017;31(3):260–74.
57. Steele CD, Pillay N, Alexandrov LB. An overview of mutational and copy number signatures in human cancer. J Pathol. 2022;257(4):454–65.
58. Zhao X, Lei Y, Li G, Cheng Y, Yang H, Xie L, et al. Integrative analysis of cancer driver genes in prostate adenocarcinoma. Mol Med Rep. 2019;19(4):2707–15.
59. Isaacsson Velho P, Fu W, Wang H, Mirkheshti N, Qazi F, Lima FAS, et al. Wnt-pathway activating mutations are associated with resistance to first-line abiraterone and enzalutamide in castration-resistant prostate cancer. Eur Urol. 2020;77(1):14–21.
60. Lu Y, Nie D, Witt WT, Chen Q, Shen M, Xie H, et al. Expression of the fat-1 gene diminishes prostate cancer growth in vivo through enhancing apoptosis and inhibiting GSK-3 beta phosphorylation. Mol Cancer Ther. 2008;7(10):3203–11.
61. van Kempen LC, Redpath M, Elchebly M, Klein KO, Papadakis AI, Wilmott JS, et al. The protein phosphatase 2A regulatory subunit PR70 is a gonosomal melanoma tumor suppressor gene. Sci Transl Med. 2016;8(369):369ra177.
62. Lynch HT, Snyder CL, Shaw TG, Heinen CD, Hitchins MP. Milestones of Lynch syndrome: 1895–2015. Nat Rev Cancer. 2015;15(3):181–94.
63. Albacker LA, Wu J, Smith P, Warmuth M, Stephens PJ, Zhu P, et al. Loss of function JAK1 mutations occur at high frequency in cancers with microsatellite instability and are suggestive of immune evasion. PLoS ONE. 2017;12(11): e0176181.
64. Chen W, Hoffmann AD, Liu H, Liu X. Organotropism: new insights into molecular mechanisms of breast cancer metastasis. NPJ Precis Oncol. 2018;2(1):4.
65. Risbridger GP, Davis ID, Birrell SN, Tilley WD. Breast and prostate cancer: more similar than different. Nat Rev Cancer. 2010;10(3):205–12.
66. Yarchoan M, Albacker LA, Hopkins AC, Montesion M, Murugesan K, Vithayathil TT, et al. PD-L1 expression and tumor mutational burden are independent biomarkers in most cancers. JCI Insight. 2019;4(6):e126908.
67. Abida W, Cheng ML, Armenia J, Middha S, Autio KA, Vargas HA, et al. Analysis of the prevalence of microsatellite instability in prostate cancer and response to immune checkpoint blockade. JAMA Oncol. 2019;5(4):471–8.
68. Rizvi NA, Hellmann MD, Snyder A, Kvistborg P, Makarov V, Havel JJ, et al. Cancer immunology. Mutational landscape determines sensitivity to PD-1 blockade in non-small cell lung cancer. Science. 2015:348(6230):124–8.
69. Chan TA, Yarchoan M, Jaffee E, Swanton C, Quezada SA, Stenzinger A, et al. Development of tumor mutation burden as an immunotherapy biomarker: utility for the oncology clinic. Ann Oncol. 2019;30(1):44–56.
70. Antonarakis ES, Piulats JM, Gross-Goupil M, Goh J, Ojamaa K, Hoimes CJ, et al. Pembrolizumab for treatment-refractory metastatic castration-resistant prostate cancer: multicohort, open-label phase II KEYNOTE-199 study. J Clin Oncol. 2020;38(5):395–405.
71. Kwon ED, Drake CG, Scher HI, Fizazi K, Bossi A, van den Eertwegh AJ, et al. Ipilimumab versus placebo after radiotherapy in patients with metastatic castration-resistant prostate cancer that had progressed after docetaxel chemotherapy (CA184-043): a multicentre, randomised, double-blind, phase 3 trial. Lancet Oncol. 2014;15(7):700–12.
72. Petrylak DP, Ratta R, Matsubara N, Korbenfeld EP, Gafanov R, Mourey L, et al. Pembrolizumab plus docetaxel for patients with metastatic castration-resistant prostate cancer (mCRPC): randomized, double-blind, phase 3 KEYNOTE-921 study. J Clin Oncol. 2023:41(6_suppl):19-.

Publisher's Note